X-613-67-132

NASA TM X- 55791

SOME EFFECTS OF MEV ELECTRONS ON THE OGO II (POGO) AIRGLOW PHOTOMETERS

BY
EDITH I. REED
WALTER B. FOWLER
CHARLES W. AITKEN
JEAN FRANCIS BRUN

MARCH 1967

GODDARD SPACE FLIGHT CENTER
GREENBELT, MARYLAND

1134

SOME EFFECTS OF MEV ELECTRONS ON THE OGO II (POGO) AIRGLOW PHOTOMETERS

Edith I. Reed
Walter B. Fowler

Goddard Space Flight Center
Greenbelt, Maryland

Charles W. Aitken
Vitro Corporation of America
Vitro Services Division
Fort Walton Beach, Florida

Jean Francis Brun

Centre National de la Recherche Scientifique
Fort de Verrieres
Verrieres le Buisson (Seine et Oise)

Paris France

TABLE OF CONTENTS

LIST OF ILLUSTRATIONS

ABSTRACT

After noting the high levels of background current in the Main Body Airglow Photometer on OGO-II, a Polar Orbiting Geophysical Observatory, a series of laboratory tests were made to indicate the sources of interference and methods of prevention. Tests with 2.6 MeV electrons confirmed that such electrons in space could account for the observed signals. Other tests were made which (1) showed that the most sensitive portion of the photometer was the cathode-window combination in the photomultiplier, (2) indicated the effectiveness of various methods of shielding, and (3) studied the presence and decay time of radiation-induced phosphorescence. Further laboratory tests confirmed that a similar OPEP photometer on the same satellite, with a different photomultiplier, a more limited spectral range, and greater shielding, was relatively insensitive to the same environment.

INTRODUCTION

Two photometers for the purpose of monitoring the earth's airglow in several different spectral regions were placed in orbit October 14, 1965 on the second Orbiting Geophysical Observatory, OGO-II. The orbit was nearly polar (87.4° inclination) with apogee near 1500 km and perigee near 400 km. One instrument, the Main Body photometer, measured the airglow below the spacecraft through six different optical filters and above through one filter. The second instrument, the OPEP photometer, scanned the airglow horizon at 6300 A.

It was soon noted that there was a large variable background (dark current) in the Main Body photometer data. The effect was largest at low latitudes when at altitudes near 1500 km, with additional relatively narrow maxima between 50° and 60° geomagnetic latitude. These corresponded to the lower part of the inner zone of trapped radiation and the low altitude portions of the outer zone respectively. At the same locations, the background current in the OPEP photometer data also increased, but the effect was about five orders of magnitude less than in the Main Body data.

It is the purpose of this report to summarize the laboratory data that was accumulated that had some bearing on this problem. Both the tests made prior to flight and the special tests made to identify the problems on OGO-II are described. A thorough discussion and explanation of the observed effects in both flight and laboratory data is to be the subject of a later report.

OBSERVED EFFECTS OF TRAPPED RADIATION

The Main Body photometer was located such that it looked through openings on both the skyward and the earthward side of the spacecraft, as shown in Figure 1. The photometer used a single photomultiplier with an arrangement of mirrors and filters such that various wavelength regions between 2500 and 6400 A were observed successively. The photomultiplier is an EMR Type 541E-05M, a one-inch diameter end-on tube with a tri-alkali cathode on a sapphire window. The multiplier was of the venetian blind type with silver-magnesium dynodes. It was sealed in a fiberglass cylinder with silicone rubber, and mounted in a magnesium housing in the photometer. The internal arrangement of the photometer is shown in Figure 2. The external windows were Corning 7940 (UV grade) and the lenses were of Suprasil (quartz). Between the objective lens and the external window of both the earth (+Z) and anti-earth (-Z) directions was a shutter of the leaf type. The mirrors were beryllium with a front surface coating of aluminum over Kanigen. The filters were of the interference type with appropriate blocking glasses.

Typical shielding to the photomultiplier that was provided by the spacecraft is indicated in Figure 3, which shows the amount of material between the photomultiplier

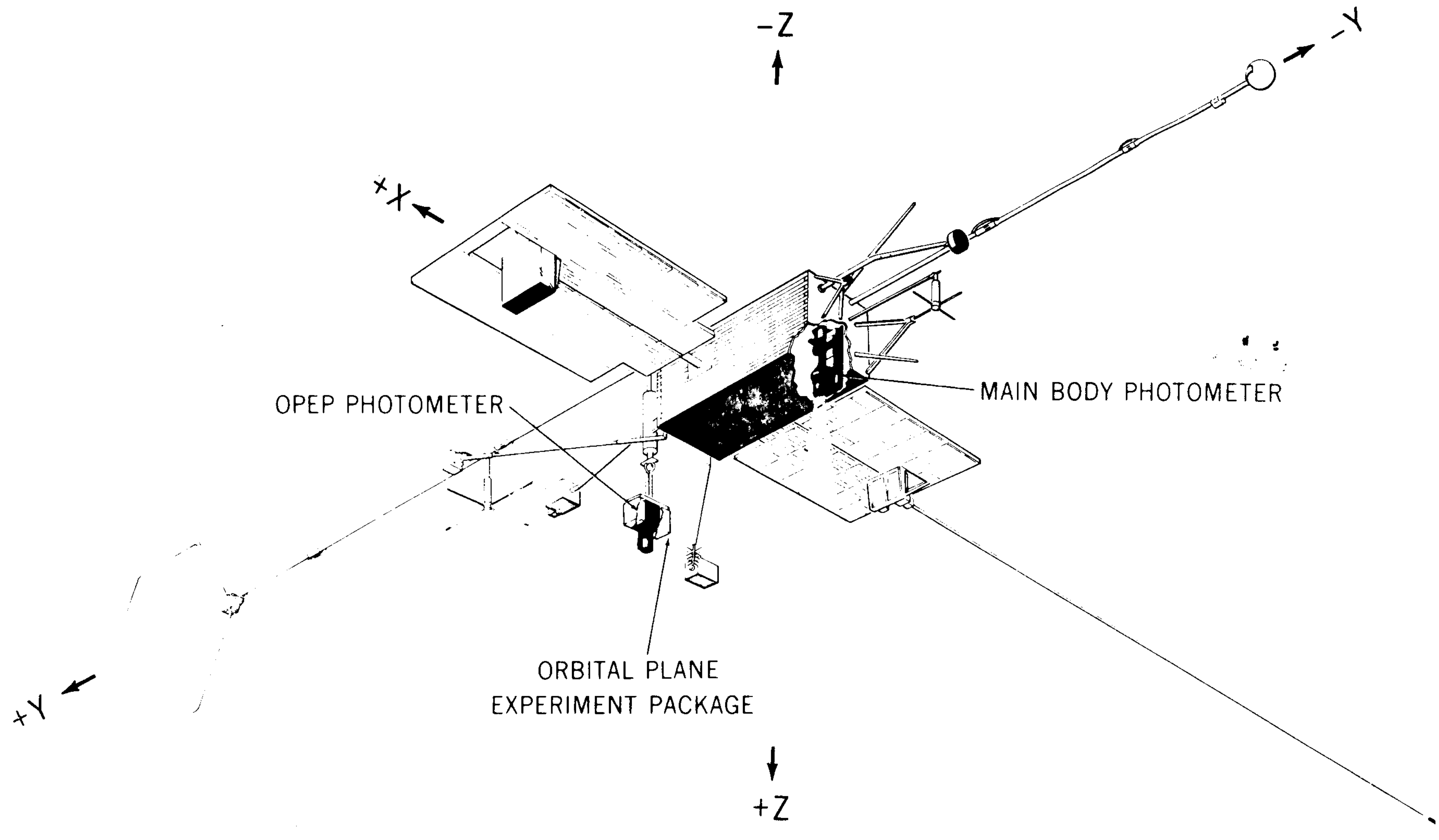

Fig. 1 - The location of the Main Body and OPEP photometers in the spacecraft. When properly oriented, the +Z axis pointed toward the center of the earth, and the -Y axis toward the sun. Shading indicates the fields of view of the photometers.

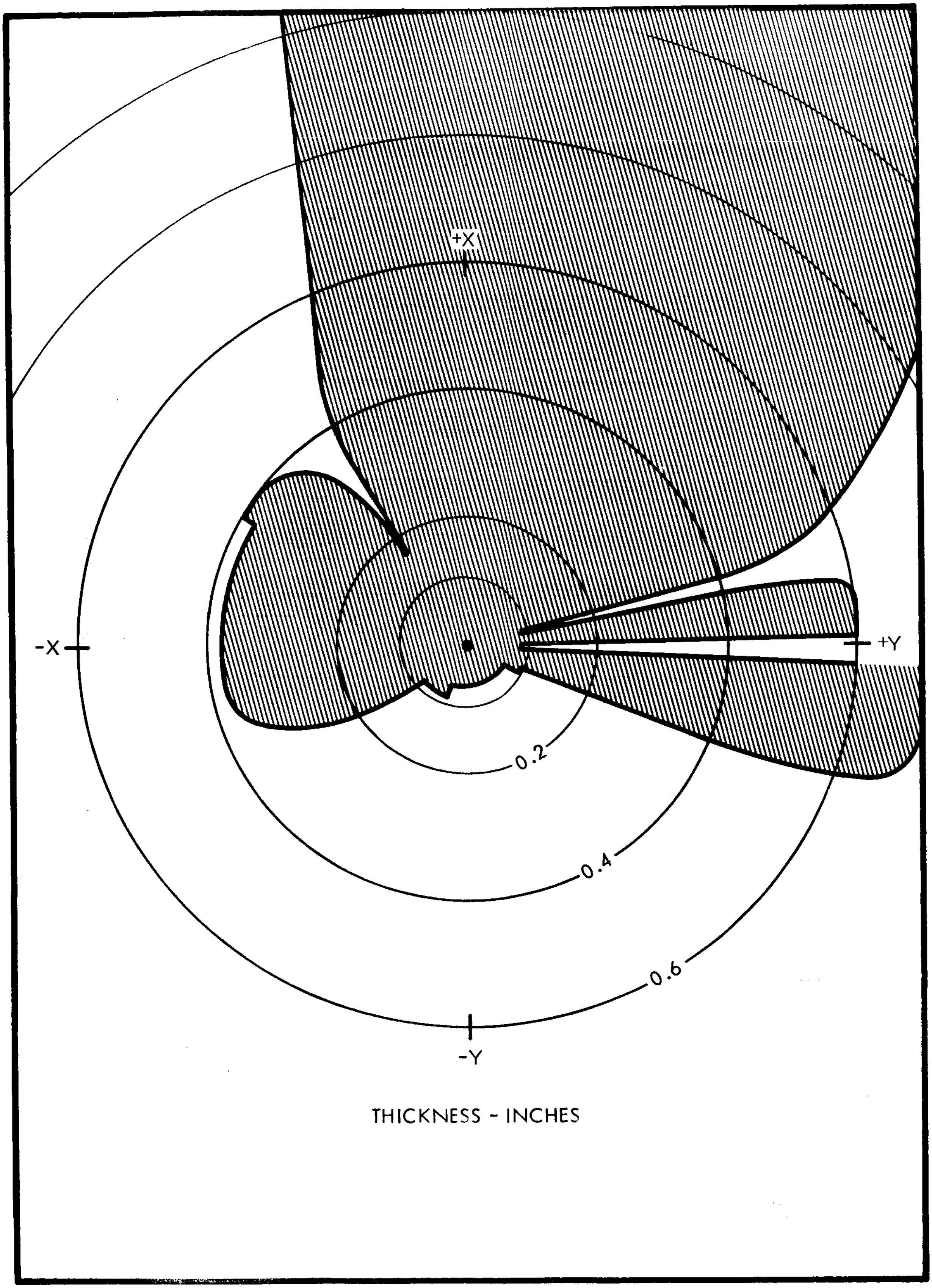

Fig. 3 - The material in the X-Y plane of the spacecraft between the photomultipliers and space. Most of the material is aluminum, and the dimensions shown include the .040" thick magnesium housing around the photomultiplier.

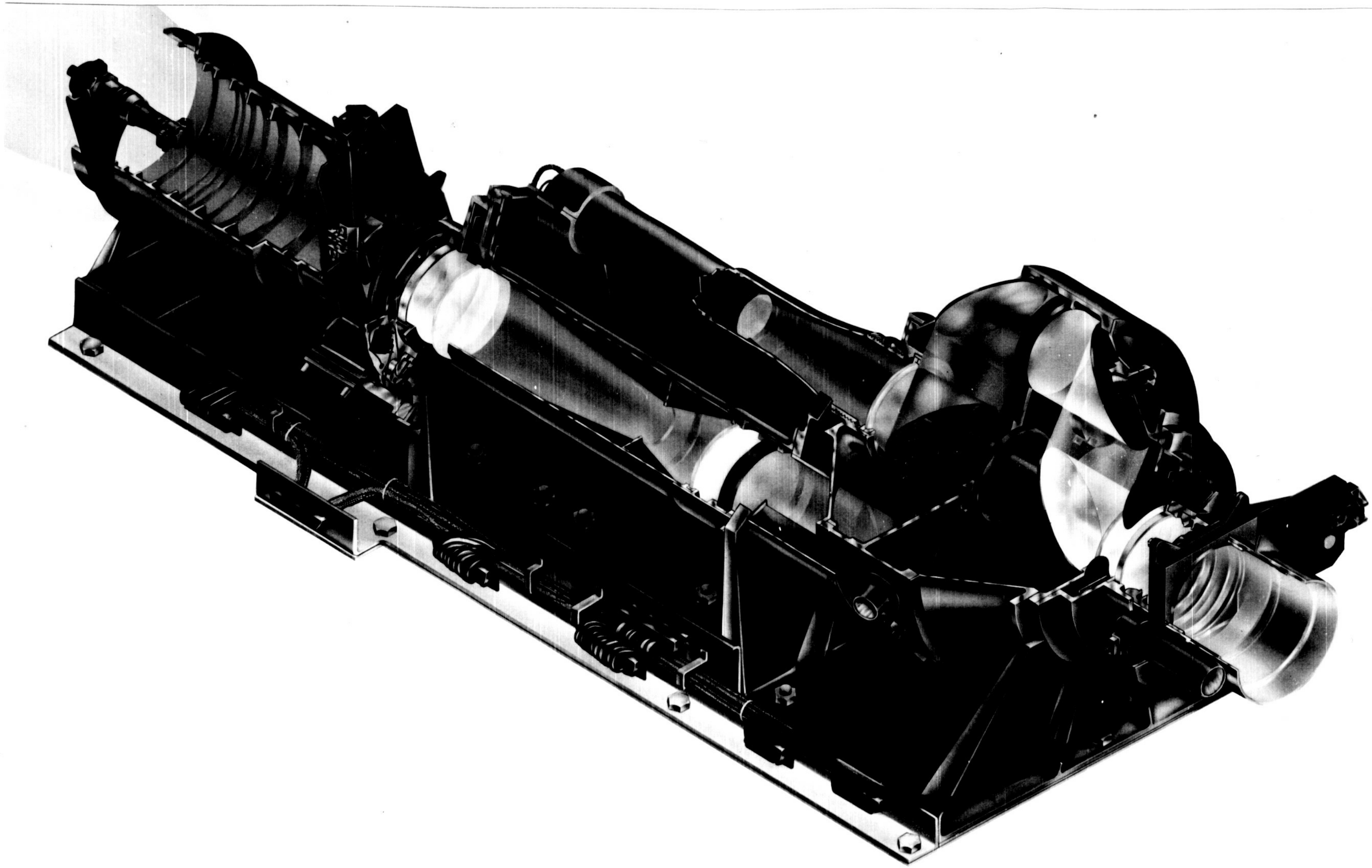

Fig. 2 - A cut-away view of the Main Body Photometer with shading added to indicate the light paths.

and outer space in the X-Y plane of the spacecraft. In other planes, the shielding is greater than the minimum thickness in the X-Y plane.

The Main Body photometer was operated with a high voltage power supply set at 2900 v , resulting in a multiplier gain of 2.7×10^6. The anode current was sensed with dc electrometer circuitry and converted to appropriate levels for telemetry. The design included a feedback loop so that when the anode current rose above 4×10^{-7} amp, a signal was generated which decreased the voltage output of the high voltage power supply, reducing the gain of the multiplier, and limiting the anode current to about 5×10^{-7} amp. A block diagram of the photometer is shown in Figure 4.

In orbit, the background current, that is, the current when the shutters were closed, ranged from a minimum of 5×10^{-16} amp from the photocathode to occasionally more than the full scale value of 3.3×10^{-9} amp. Not infrequently, this was orders of magnitude more than the current from the light we were attempting to measure. This extraneous current was not a simple increase in dark current level, but consisted of a multitude of pulses and tended to persist after the radiation levels had decreased.

It was noted that the output of the high voltage power supply increased with time for both the Main Body and OPEP photometers. It was concluded that this was due to radiation

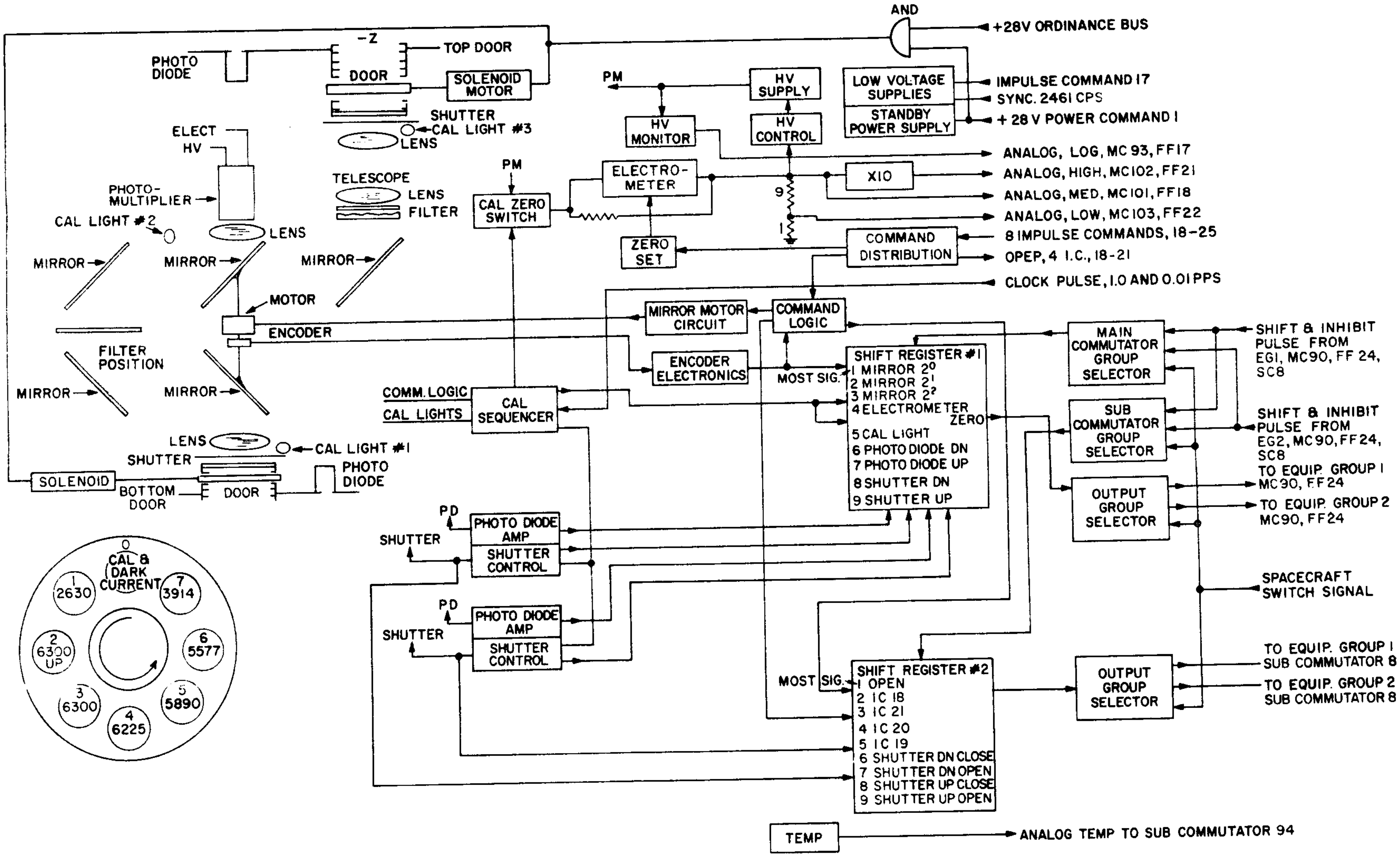

MAIN BODY PHOTOMETER

Fig. 4 - A block diagram showing the principal mechanical and electrical features of the Main Body Photometer.

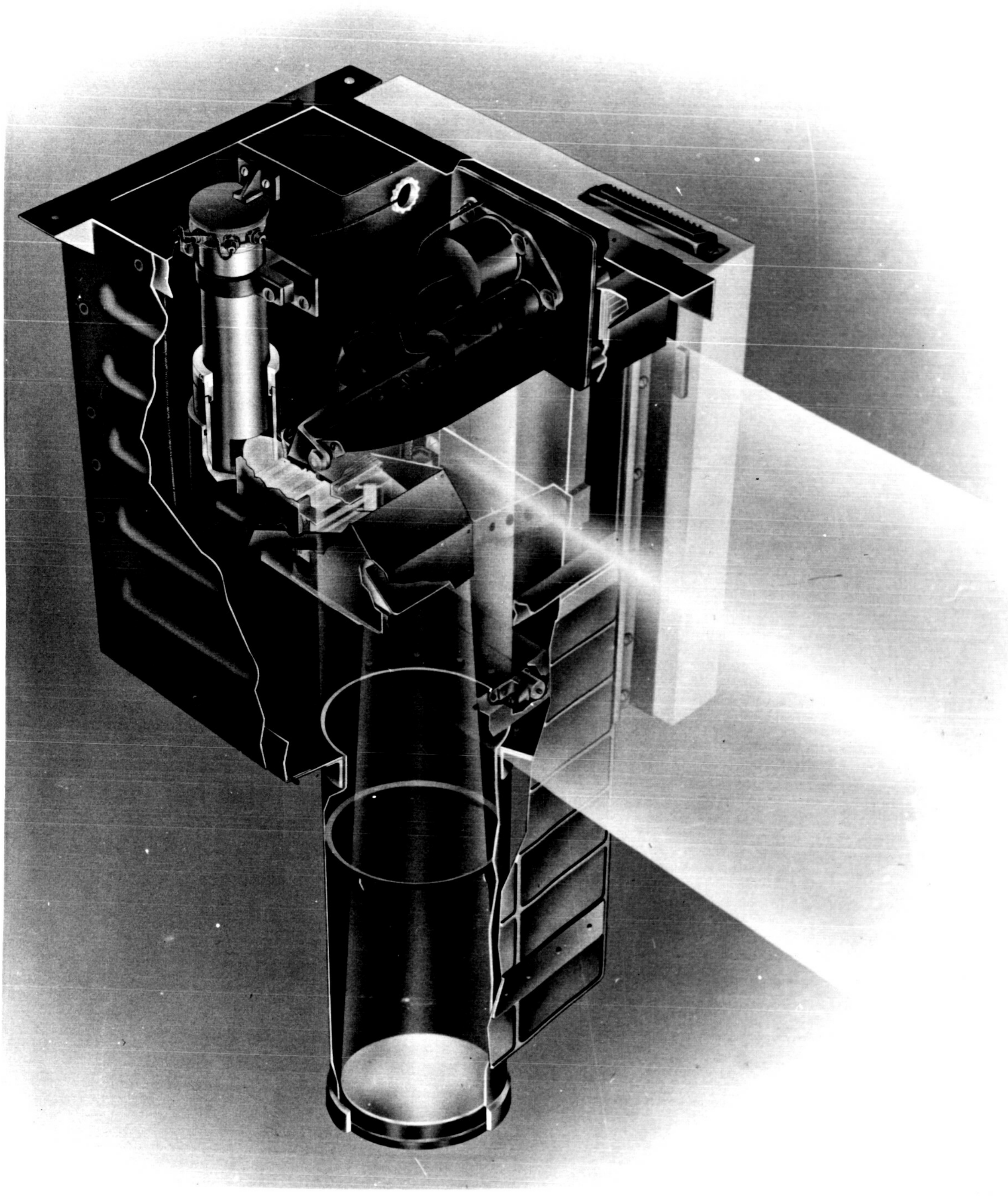

Fig. 5 - A cut-away view of the OPEP photometer with shading added to indicate the light path.

damage to a transistor resulting in a change of beta in the amplifier controlling the power supply.

The only other effect of radiation noticed on the Main Body Photometer was in the circuitry for control of the shutters. Apparently the background current in a photodiode (Texas Instrument Type 2175) increased appreciably, so that occasionally the circuit would close the shutters, even though external light levels were well within the range of the photomultiplier.

The OPEP photometer (see Figures 5 and 6) was for the purpose of measuring the altitude distribution of the red atomic oxygen airglow at 6300 A. This instrument was located in the Orbital Plane Experiment Package (OPEP) and scanned across the earth's horizon. (See Figure 1.)

In orbit, unlike the Main Body photometer, the presence of energetic particles resulted in a current of no more than 6×10^{-15} amp in terms of photocathode current from the OPEP photometer. This was probably due to one or a combination of several things: (a) the use of a side window photomultiplier (EMR Type 641E) in which the optical coupling between the window and the cathode is inefficient, the cathode being behind but not on the window, (b) window material of a glass (CS-7056) which absorbs in the ultraviolet region where Cerenkov radiation is a maximum, (c)

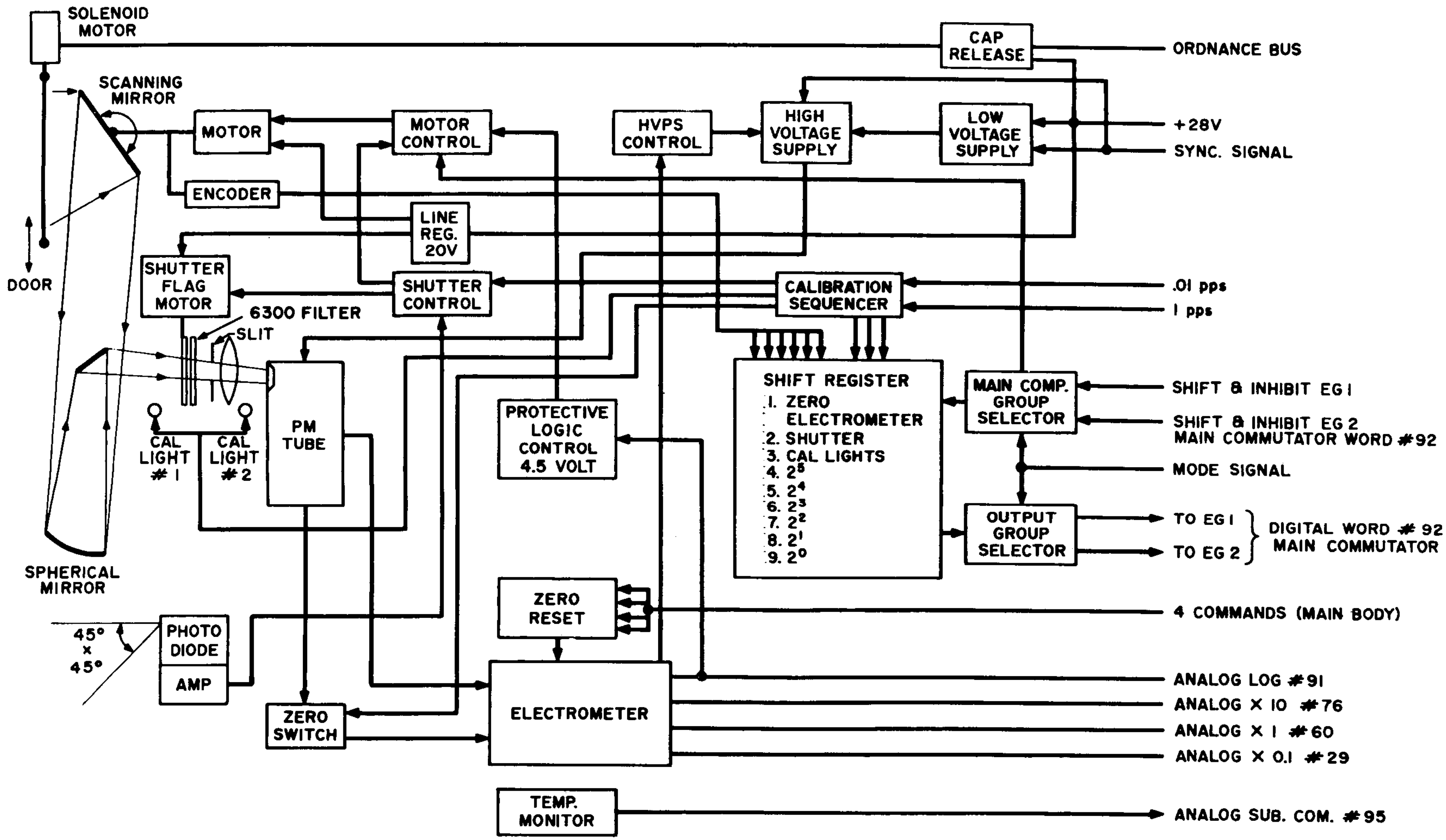

OPEP PHOTOMETER

Fig. 6 - A block diagram showing the principal mechanical and electrical features of the OPEP photometer.

dynodes of CuBe instead of AgMg, and (d) shielding of the photocathode with .12 to .20 inches of aluminum over .08 inch of tungsten, in addition to shielding provided by the remainder of the photometer and OPEP package.

After a look at the data obtained during the first ten days in orbit, it was obvious that for OGO-D, steps should be taken to reduce the response of the Main Body photometer to energetic particles. Laboratory experiments described in this report were then performed to assist in the redesign of the OGO-D photometer. These efforts were limited since decisions had to be made and implemented in a matter of a few months.

TESTS AT GRUMMAN AIRCRAFT CORPORATION, NOVEMBER 1965

In order to investigate the effects of energetic electrons on the Orbiting Astronomical Observatory (OAO) star tracker, a Van de Graaff accelerator at the Grumman Aircraft Corporation at Bethpage, New York was used. Studies by OAO Project personnel had indicated that the effects of trapped radiation of the inner artificial belt could be simulated by a monoenergetic beam of electrons at 2.6 MeV. Reference 1, discussing this electron belt in connection with OGO I, launched Sept 5, 1964, gives a flux for the center of the belt of 10^8 electrons/cm^2 sec with energies greater than 0.5 MeV. The energy spectrum is such that the number of electrons with energies greater than 6 MeV is negligible. Because of certain similarities in orbit and technique between the OAO star tracker and the OGO-II airglow photometers, we were invited to test duplicates of the OGO-II photometers in order to see if the effects observed in orbit could be reproduced at this facility.

For these tests, the "optical models" of the photometers were used. These were similar to the photometers in OGO-II with minor differences in the mechanical mechanisms, in the design of the digital circuitry, and in various voltage settings. Compromises made during their construction and testing precluded them from being of flight quality. Table I gives a comparison of the characteristics of the

TABLE I

Main Body Photometer	Optical Model	OGO-II
Normal level of high voltage (anode current less than 4×10^{-7} amp)	-2400 v	-2900v
Minimum level of high voltage (anode current about 5×10^{-7} amp)	-1000 v	- 960 v
* Gain at normal high voltage	3.3×10^{5}	2.7×10^{5}
* Gain at minimum high voltage (est.)	3.5×10^{2}	1.5×10^{2}
Dark current (anode current at normal high voltage)	8.7×10^{-10} amp	1.5×10^{-10} amp
Sensitivity at normal high voltage (amperes of anode current per Rayleigh)		
Line at 6300 A	1.75×10^{-11}	5.86×10^{-11}
Line at 5896 A	2.38×10^{-11}	7.72×10^{-11}
Line at 5577 A	2.94×10^{-11}	1.01×10^{-10}
Line at 3914 A	4.88×10^{-11}	1.39×10^{-10}
continuum between 2530 and 2730 A (amperes of anode current per Rayleigh per 100A)	8×10^{-12} (est.)	2.48×10^{-11}

* Based on manufacturer's curve before the tube was potted.

Main Body optical model with that of the OGO-II instrument.

The photometers were placed in a cylindrical vacuum tank about three feet in diameter. The tank was pumped with mechanical and oil diffusion pumps (no cold trap) and all tests were conducted at pressures between 1×10^{-4} and 1×10^{-5} mm Hg. The photometer to be tested was mounted at one end of the tank on a plate which was perpendicular to the electron beam, resulting in an arrangement as illustrated in Figure 7. The electron beam in the vicinity of the photometer had a diameter of ten inches and a flux density, as measured with a Faraday cup, which could be set in the range between 6×10^5 and 1.8×10^8 electrons cm^{-2} sec^{-1}. The technique used to adapt the Van de Graaff facility for these environmental studies is described in Reference 2.

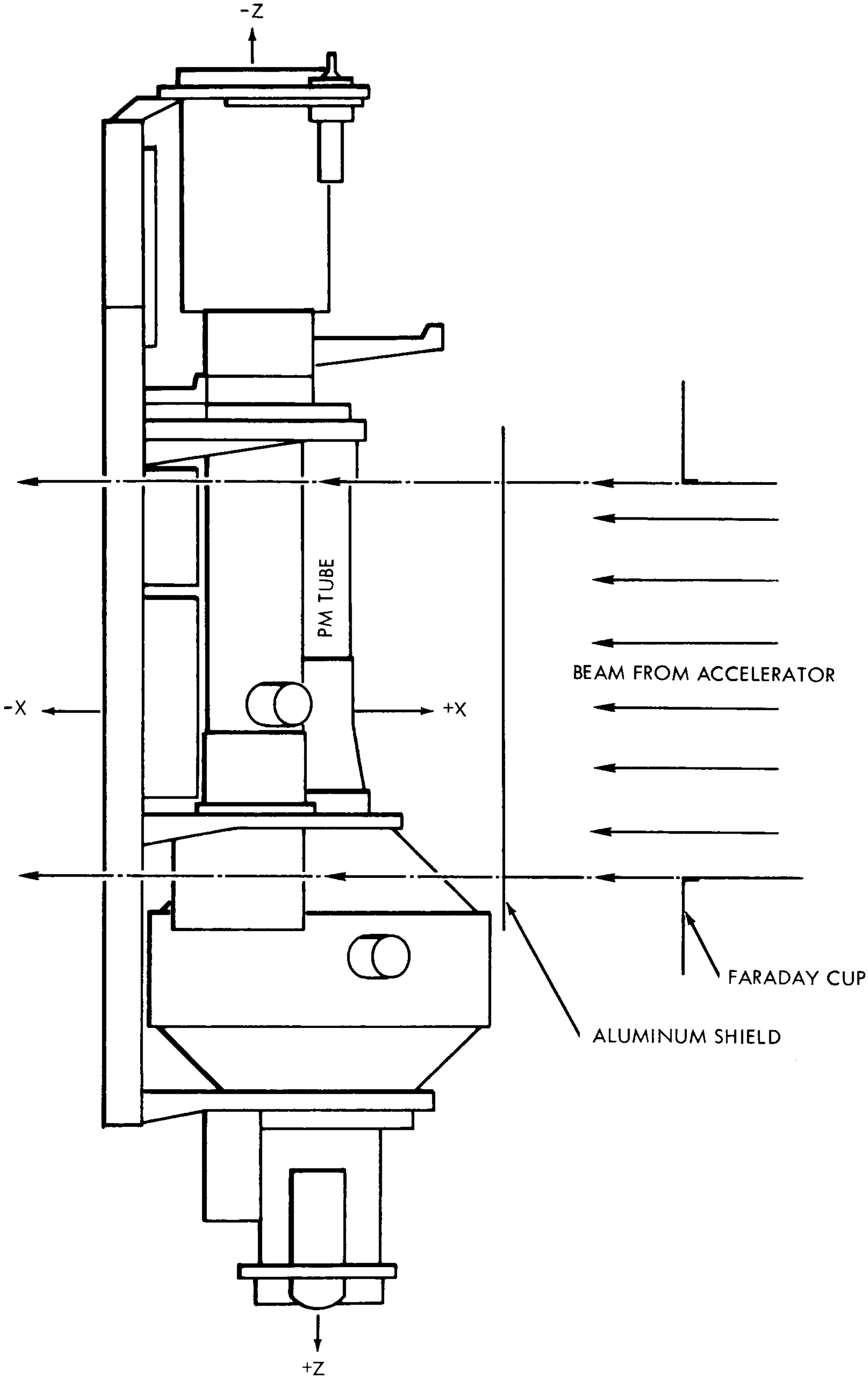

Fig. 7 - Location of the electron beam from the Van de Graaff accelerator with respect to the Main Body photometer under test. The arrows indicate the direction of the corresponding spacecraft coordinates.

The effectiveness of aluminum shielding

Large pieces of aluminum sheet of various thicknesses were placed in the path of the electron beam as indicated in Figure 7. The increase of anode current from the photometer divided by the gain of the multiplier is arbitrarily regarded as due entirely to photoelectrons. This photoelectron current divided by the flux of the beam is taken as a measure of the response of the photometer to energetic particles. As might be expected, the response is an exponential function of the thickness of the shielding, and is shown in Figure 8. The data upon which this graph is based is given in Table 1 of the Appendix.

At this point it was interesting to cross check the Van de Graaff as a simulator of the inner artificial belt. Since the optical model had about 1/3 the sensitivity of the instrument in orbit, the equivalent cathode current of the belt might be taken as 1.1×10^{-9} amp. Letting 0.08 in. aluminum simulate the spacecraft skin and using Appendix Table 1 and Figure 8, the background current of the belt is reached at 5×10^{7} electrons/cm^2 sec, monoenergetic at 2.6 MeV. This a in fair agreement with the flux of 10^{8} electrons/cm^2 sec with energies greater than 0.5 MeV, calculated for OGO-I. If belt decay is taken into account, the agreement is surprisingly good.

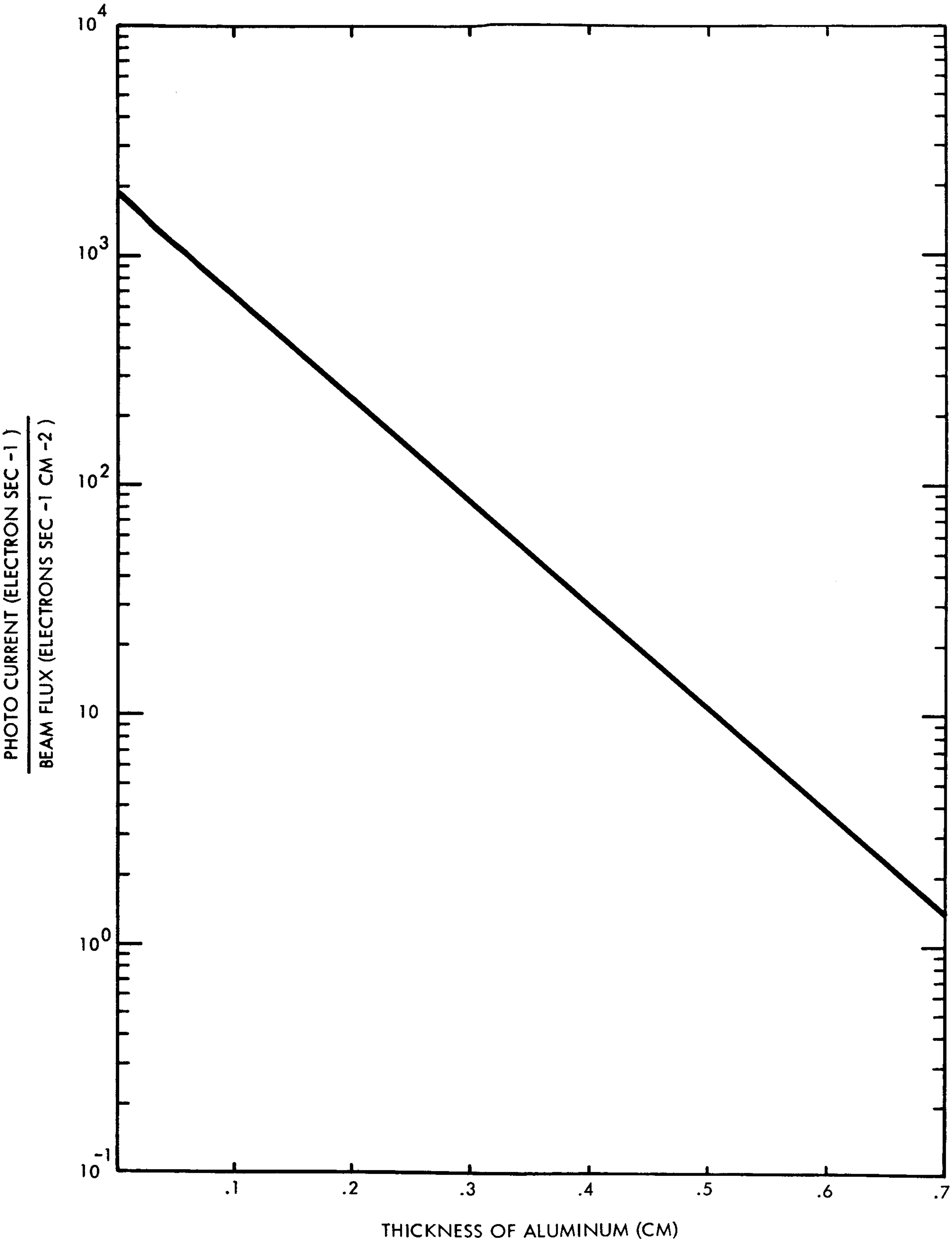

Fig. 8 - Effect of aluminum shielding upon the response of the Main Body photometer to 2.6 Mev electrons.

The luminescence of the Optics

In order to determine whether the extraneous background current was due to the effects of the electron beam on the photomultiplier or to a luminescence of the field lens, an aluminum disk, 1/8 inch thick, was placed as a light stop, as shown in Figure 9. To minimize the effects in the photomultiplier, a 1/4 inch thick cylinder of lead was placed as shown. To represent the shielding provided by the spacecraft, a 1/16 inch thick aluminum sheet was placed in the path of the beam. Measurements made with and without the light stop (see Table 2 of the Appendix) indicated that the photocurrent due to luminescence of the lens and its immediate vicinity was negligible.

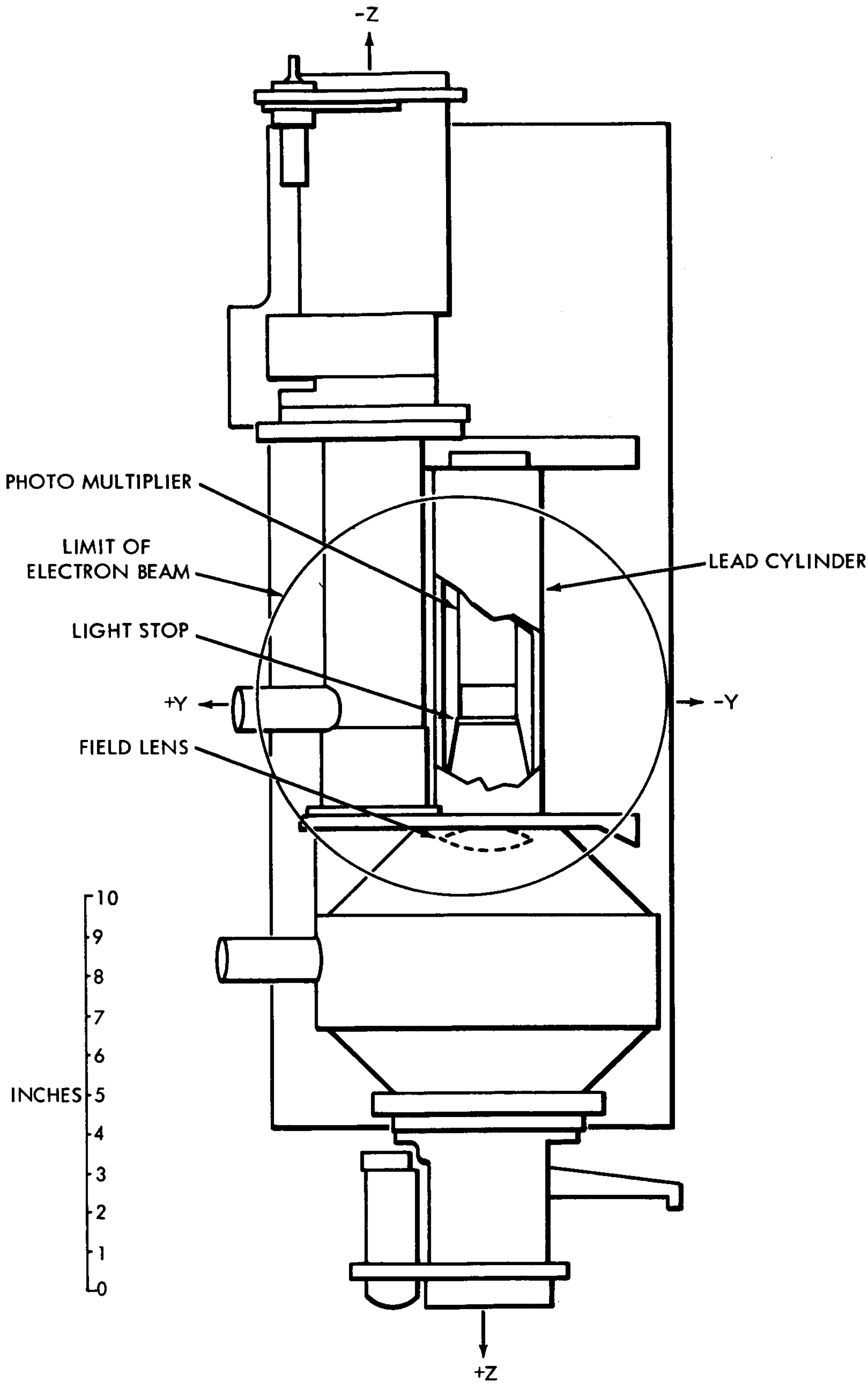

Fig. 9 - Placement of light stop and lead shielding so as to detect luminescence of the field lens.

Response of the photomultiplier

The results of the preceding test indicated that suprasil field lens was not a major source of light when under particle irradiation. The inflight calibration cycle included a zero level which measured the output of the electrometer and associated electronics without the signal input from the photomultiplier. This zero level remained constant under all conditions, thus eliminating the electronics circuitry as a radiation sensitive area. Since each filter is made with a different type of glass, and in one position, the "filter" is a solid metal plate, it would be expected that the response would be quite dependent on mirror position if the filters or the objective lens and window were important sources of light. Data from OGO-II indicated that the value of the extraneous background current was independent of mirror position. Hence the sensitive component must be the photomultiplier.

To indicate which part of the photomultiplier was most sensitive, i.e., the dynodes or the photocathode, the following tests were performed.

As in the preceding test, the light stop remained in place in front of the photomultiplier and a 1/16 in. sheet of aluminum was used to simulate the shielding provided by the spacecraft. A lead sheet 1/4 inch thick was placed around the photomultiplier in the various positions indicated in Figure 10. The results are as follows (also see Table 3 in the Appendix)

Portion covered by lead	Photoelectrons/electrons cm^{-2}
Cathode, dynodes #1 and #2	2.0
Cathode, dynode #1	2.0
Cathode	24
Dynode #1 and #2	530

From these tests, it is apparent that the bulk of the response of the photomultiplier is due to the photocathode and the window upon which it is deposited. In our experiments, no effort was made to further isolate the contribution between window and cathode. It should be noticed that for the more common soda lime glass envelopes the luminescence of the glass proved to be the major contributer under γ and x-ray excitation (Ref. 3).

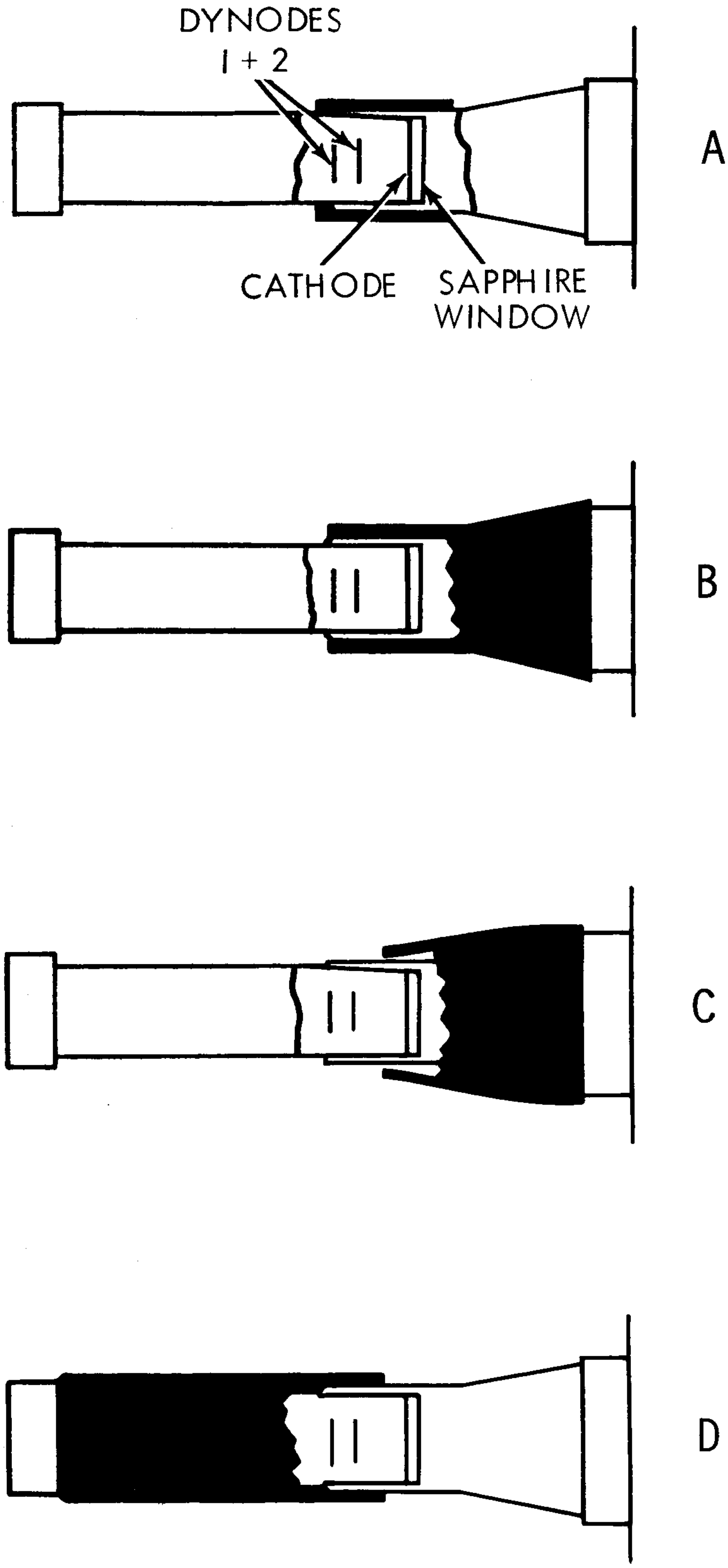

Fig. 10 - Placement of a lead shield over various parts of the photomultiplier.

Various Shielding Configurations

The next problem was to develop some insight as to what type of shielding was both effective and light in weight. It was noted from the comparison of the results of the earlier test using aluminum and lead, the aluminum and lead were about equal in effectiveness for equal thicknesses of material. It was suggested that a combination of high and low density materials would be more effective than either alone. With the light stop still in place, tests of shielding as indicated in Figure 11 were made: (Detailed data is in Table 4 of the Appendix).

	SHIELDING	PHOTOCATHODE CURRENT / BEAM FLUX
A.	.062" aluminum over whole beam .062" tungsten over cathode and dynodes 1 and 2	220
B.	.062" aluminum over whole beam .125" tungsten over cathode and dynodes 1 and 2	220
C.	.062" aluminum over whole beam .125" aluminum over cathode and dynodes 1 and 2 .096" tungsten over cathode and dynodes 1 and 2	220
D.	.062" aluminum over whole beam .125" aluminum from dynode 2 to optics cage .096" tungsten over cathode and dynodes 1 and 2	1.4

The first three tests in this series show only a slight reduction in radiation induced signal below what would have been expected with a .062" aluminum shield alone. But in the fourth test, where a thick shield extended well in front

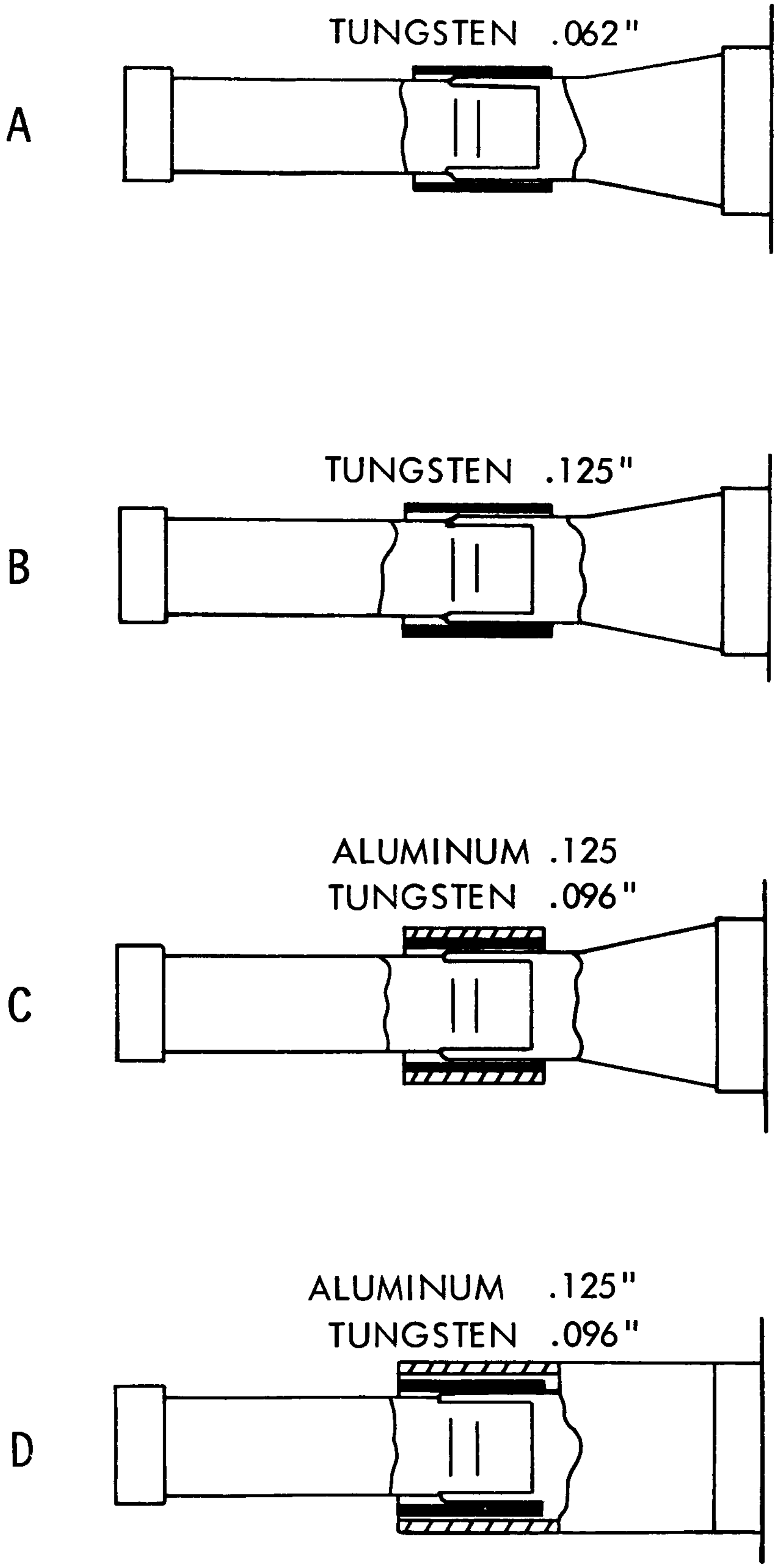

Fig. 11 - The various arrangements of shielding that were tested.

of the cathode, protecting against scattered electrons, there is a pronounced reduction in the radiation induced signal.

In addition to these tests at Grumman the GSFC Van de Graaff was used to measure the effectiveness of a quartz plate in front of the photomultiplier window. This test is discussed at the end of the section on window materials.

Response of the OPEP photometer

The Main Body photometer was removed from the tank, and tests were made with the OPEP photometer. In order to find in which direction the photometer was most sensitive to energetic electrons, each of five sides of the photometer were irradiated and the response measured. To simulate the OPEP container, a sheet of aluminum, 0.32" thick, was placed in the path of the beam, except, of course, on the side with the large open window. The results are indicated in Figure 12 where the length of the axes represents the sensitivity to energetic electrons in that direction. (Also see Table 5 of the Appendix.) Because the OPEP mounting plate is 0.5 inches thick, it is estimated that the sensitivity in that direction (-Z) is small, as indicated.

The result of this test is consistent with the observations in orbit, namely, that the response of the OPEP photometer to the trapped radiation is about four to five orders of magnitude less than for the Main Body photometer.

It was desired to measure the sensitivity to energetic electrons of photomultipliers with AgMg instead of CuBe dynodes. To do this, photomultipliers of the two types of construction

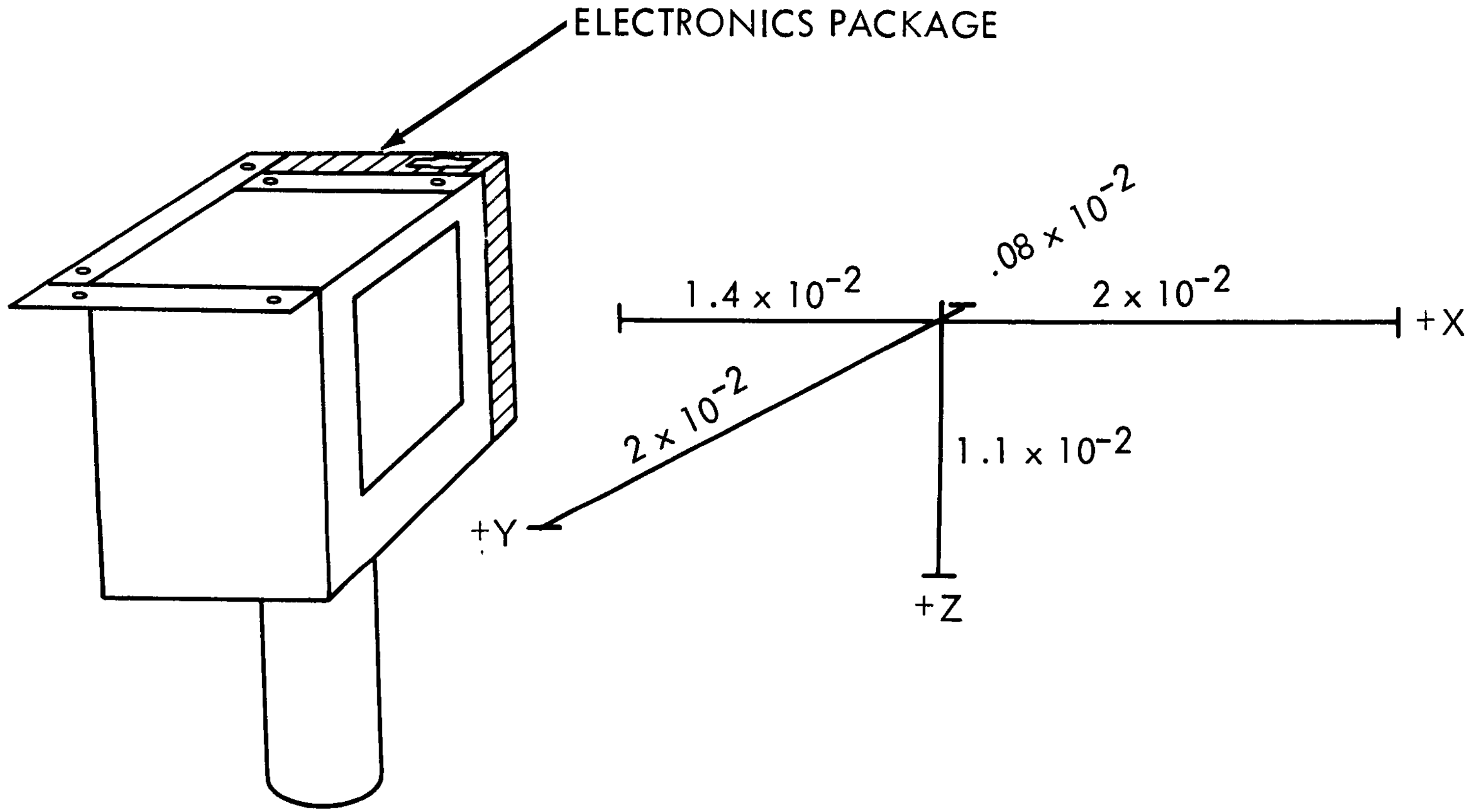

Fig. 12 - The response of the OPEP photometer to energetic particle radiation from different directions. The length of the axis represents the response. The number is the photo-current (electrons sec^{-1}) divided by the beam flux (electrons cm^{-2} sec^{-1}).

were installed in the OPEP photometer, and the sensitivity measured with the open door (+X axis) facing the beam. Two of the tubes were of the same type with CuBe dynodes and a tri-alkali cathode. The third had AgMg dynodes and a CsSb cathode. All three tubes had 14 stages and were operated with the high voltage power supply set at 1800v.

"Photocathode current", given in Table 6 in the Appendix, was obtained by dividing the measured anode current by the gain of the multiplier as measured by the manufacturer prior to potting the photomultiplier in its fiberglass sleeve. The CuBe tubes were about two years old, the AgMg tube, three years. The apparent result, that AgMg dynodes are 2 to 4 times more sensitive to energetic electrons than are CuBe dynodes, is not conclusive because part of the difference may be due to changes in gain with age and part due to the difference in cathode composition.

TESTS OF VARIOUS PHOTOTUBE WINDOW MATERIALS

As a result of the tests at Grumman Aircraft Corporation, it appeared that much of the extraneous current was due to the interaction of the energetic particles with the window material and the photocathode. As the energetic particles pass through the window, part of their energy loss appears as Cerenkov radiation and bremstrahlung; another part of their energy loss is by ionization and excitation collisions, with some of this energy appearing as fluorescence and phosphorescence. Secondary electrons and x-rays originating in nearby parts of the spacecraft would have similar effects.

While it would have been interesting to have made a thorough study of the intensity, spectra, and decay of the luminescence of various window materials irradiated by a wide spectrum of electron energies, resources were not available to do this. Hence, some early experiments involving energetic electrons were reviewed and some additional tests were made with the GSFC Van de Graaff accelerator. The pertinent results are summarized in the following section.

Excitation by electron microscope

Observations of electron excited luminescence in quartz and sapphire have been made at GSFC by A. G. Eubanks and T. D. Sciacca of the Materials Research and Development Branch. An electron microscope was used to provide a beam with a flux of 10^8 electrons cm^{-2} sec^{-1} at 50 KeV. As in

Figure 13, (also Reference 4), the sample was mounted at 45 degrees to the incident beam and the resulting luminescence was viewed by a photomultiplier tube at right angles to the electron beam. The photomultiplier viewed the sample through a quartz window in the microscope housing. Results were as follows in terms of relative intensity:

Material	Relative Luminescence
Corning 7940, uv grade	1.0
Sapphire	2.1
Suprasil	1.1

Detailed spectral measurements were not made. The photomultiplier, an EMI 6526B, with a semi-transparent CsSb cathode and a fused silica window, and the quartz window in the microscope housing restricted the observations to the wavelengths longer than 1800A. Tests with several long-pass filters showed that all of the light was at wavelengths shorter than 4100A.

When the measurement of absolute intensity was made, the quartz window was no longer available, and the samples had to be observed through a lead-doped glass window. The absolute brightness for the luminescence of sapphire between 3500 and 4100A was about 10^{-11} watts cm^{-2} $steradian^{-1}$. Tests with several short-wavelength cut-off filters showed about 60% of this energy was at wavelengths shorter than 3800A.

Excitation by radioactive beta source

A comparison between luminescence of sapphire and

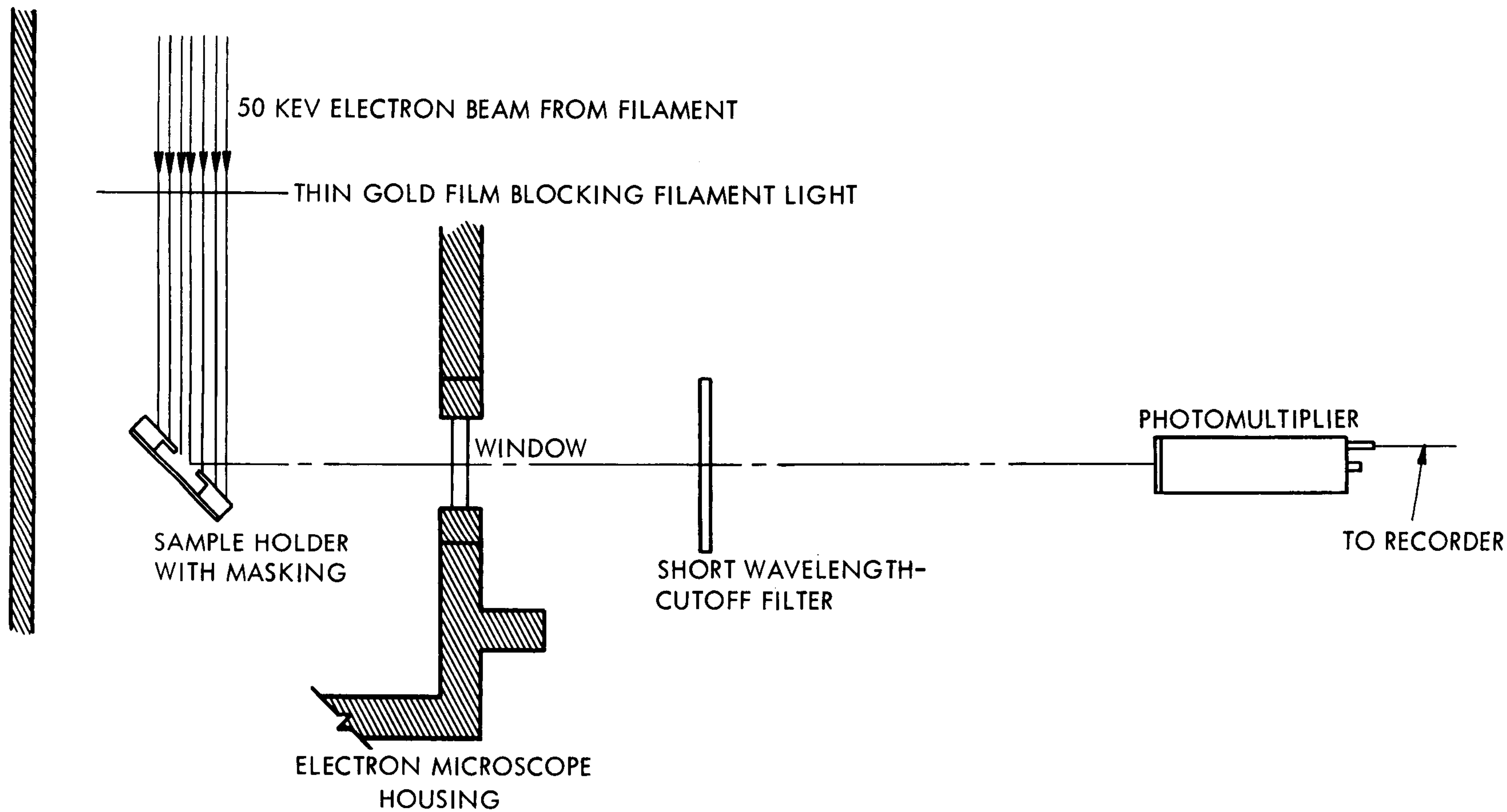

Fig. 13 - In this test arrangement, the beam of an electron microscope was used as a source of energetic particles.

suprasil can be made from an ultraviolet source used at this laboratory as an aid in low brightness calibrations (see Figure 14). The excitation is a radioactive 1 millicurie strontium-90 beta source. Maximum Sr^{90} beta energy is 545 KeV; Y^{90} beta energy is 2.26 MeV; γ strength is 1.74 MeV with a flux of 6×10^2 γ/cm^2.

When the front face of the source, 1/4 inch square, is placed behind and against suprasil or sapphire, our photometer measured the radiances as given below. Each wavelength region was measured with an interference filter, with the center wavelength and bandpass indicated. Brightness is in watts cm^{-2} steradian^{-1} per 100A.

Wavelength	Bandpass	Suprasil	Sapphire
2600A	198A	2.4×10^{-12}	1.6×10^{-11}
3914A	43A	$.90 \times 10^{-12}$	$.17 \times 10^{-11}$
5577A	50A	$.26 \times 10^{-12}$	$.018 \times 10^{-11}$
5890A	50A	$.28 \times 10^{-12}$	$.0066 \times 10^{-11}$
6225A	51A	neg.	$.28 \times 10^{-11}$
6300A	50A	neg.	$.37 \times 10^{-11}$

With an interference filter removed, the total radiance between 1800A and 6300A could be determined approximately, assuming constant spectral responsivity for the photomultiplier. The values thus obtained are 6.70×10^{-11} watts cm^{-2} steradian^{-1} for suprasil and 3.8×10^{-10} watts cm^{-2} steradian^{-1} for sapphire. The maximum brightness is apparently at wavelengths shorter than 2600A, as would be expected from theory (Ref. 5).

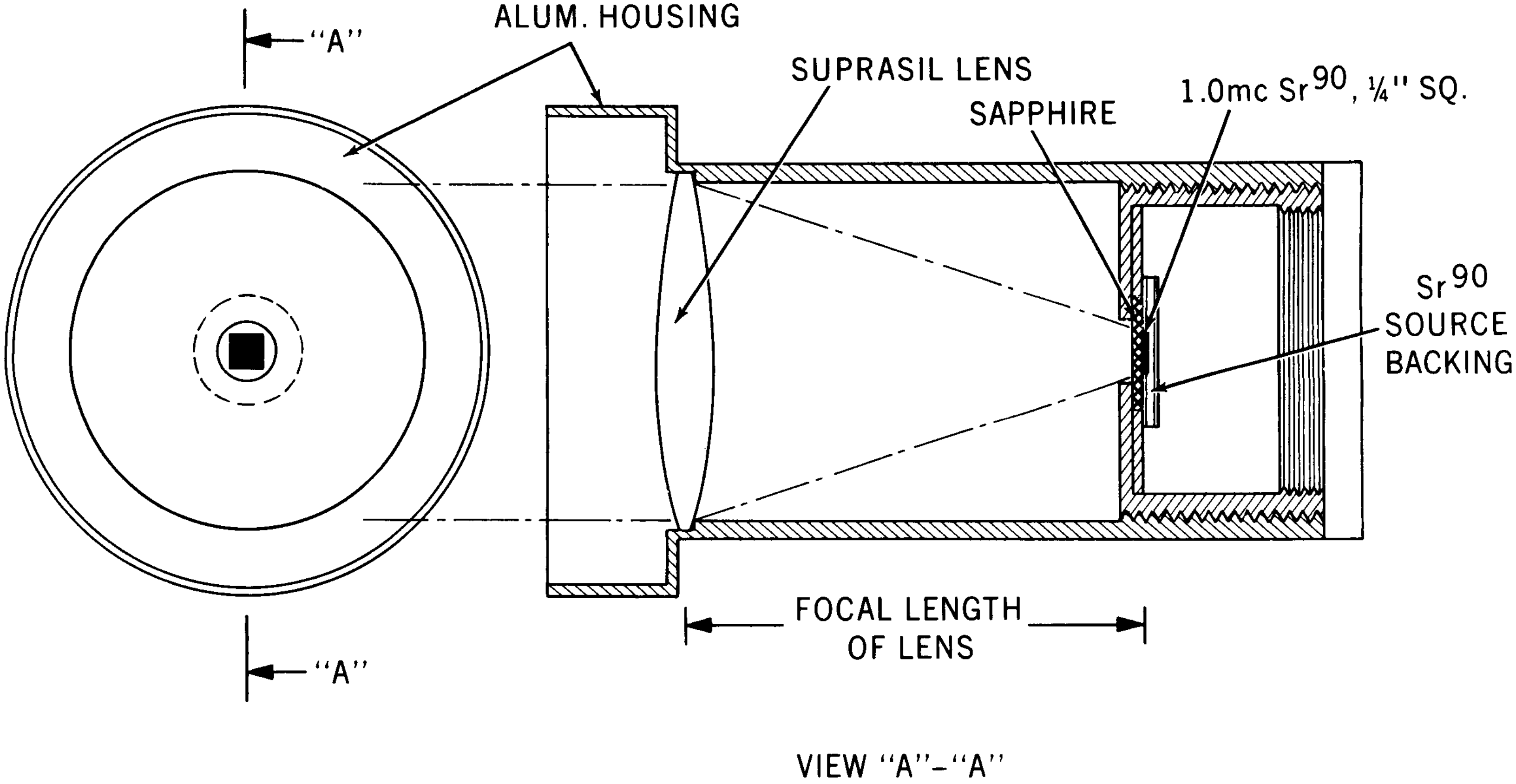

Fig. 14 - Low Brightness Ultraviolet Light Source. Electrons from the Sr^{90} incident on the sapphire cause luminescence which includes Cerenkov radiation for brightness at the short wavelengths near the transmission cut-off of the suprasil lens.

Excitation with Van de Graaff accelerator

To further investigate the luminescence of various window materials, arrangements were made to use a Van de Graaff accelerator at GSFC. The accelerator was set to produce a beam of electrons of 1.25 MeV energy, the maximum possible. The beam was directed on the samples located in a vacuum tank. A comparison of the relative brightness in the spectral region between 1600 and 6300A was made with an EMR type 541E-05M photomultiplier, also placed within the vacuum tank.

The test samples, with a metal mask of 1 cm^2 opening, were placed one at a time in the vacuum tank. (See Figure 15) Lead bricks were placed between the photomultiplier and the accelerator to reduce the background which apparently was due to stray x-rays. Three different samples of sapphire and five of quartz were tested, with the general conclusion that quartz emits about 0.7 as much light as does sapphire. For detailed data, see Table 7 of the Appendix.

When the accelerator beam was turned off, the signal decayed at a rate, which between 20 and 250 seconds can be described by a curve of the form, $I^{-0.5} = at + b$, where I is the observed apparent intensity, t is the time, and a and b are constants. The data presented in Figure 16 are typical. Since this is appreciably above the background observed when there is no sample in the holder, it cannot be a characteristic of the surroundings. All samples were washed in ethyl alcohol prior to placement in the vacuum chamber; pressures were typically in the region of 10^{-4} mm Hg. It is possible that some portion

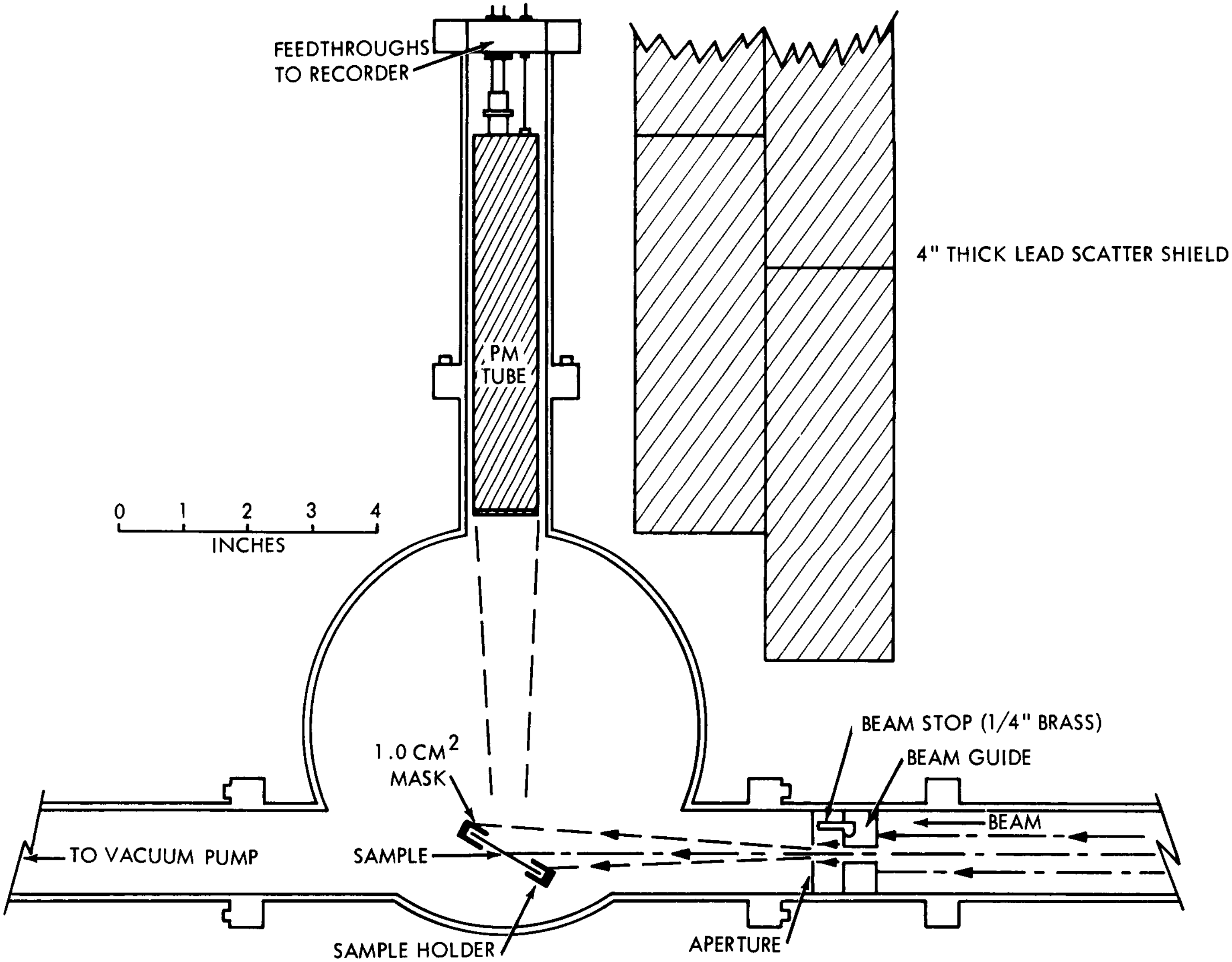

Fig. 15 - Arrangement of the samples and the photomultiplier with the GSFC Van de Graaff accelerator.

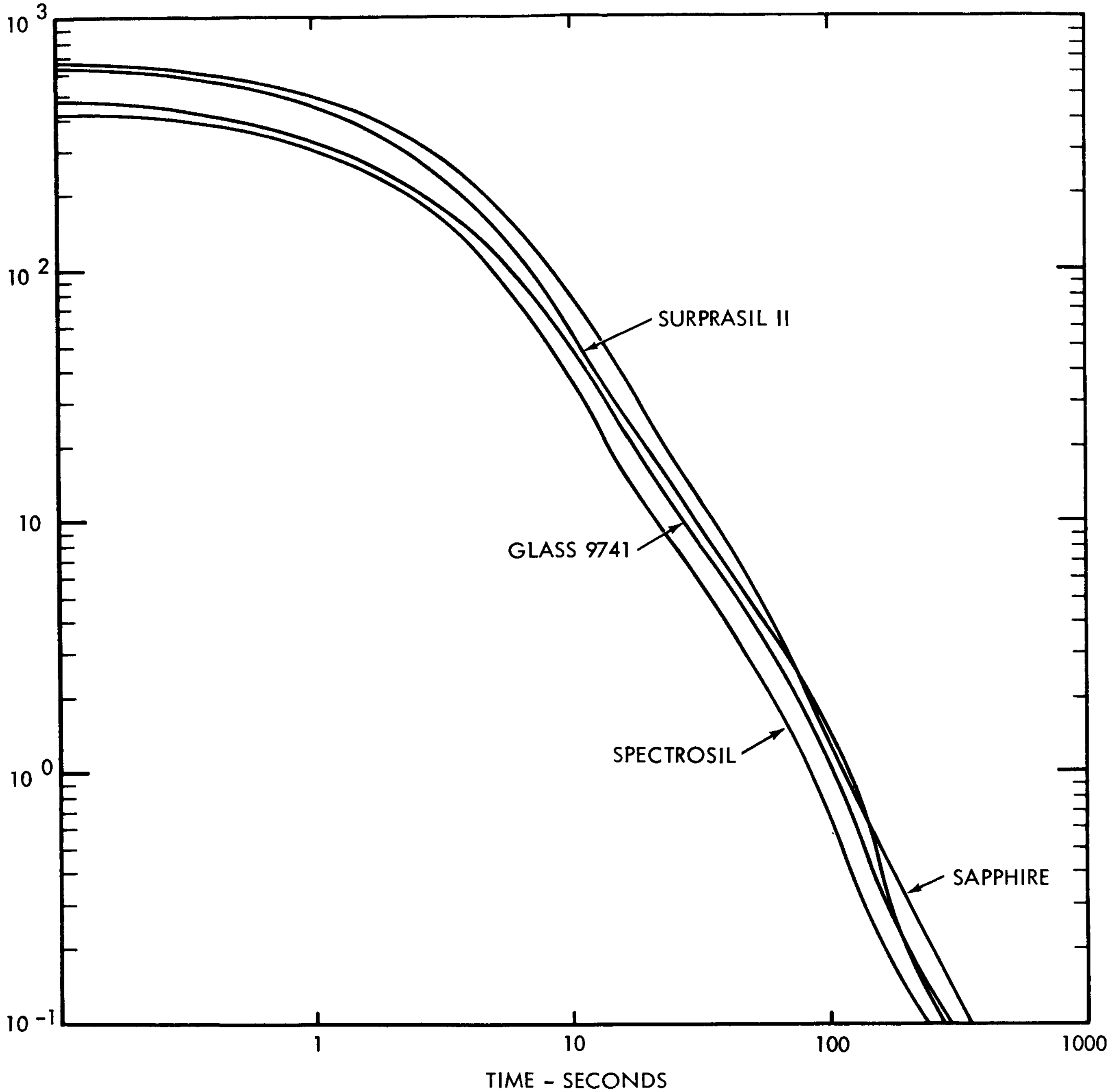

Fig 16 - The rate of decay of luminescence for various materials after turning off the electron beam of the Van de Graaff accelerator.

of the observed luminescence originated in surface films.

PERFORMANCE OF OTHER PHOTOMULTIPLIERS ON OGO SPACECRAFT

Several other photomultipliers have flown in spacecraft for various reasons. Wolff (Ref. 1) reports on an image dissector on OGO-I with a tri- alkali (S-20) cathode deposited on a thin curved window of Corning 9741 uv transmitting glass. With a minimum shielding of 1.2 gms/cm^2 he noted a maximum of 1.3×10^5 $counts/sec\text{-}cm^2$ when passing through the radiation belt. This is comparable to the response of our OPEP photometer.

Also on OGO-II were two EMR photomultipliers in the UV airglow spectrometer of Barth (Ref. 6). These photomultipliers were very similar in construction to that in our Main Body photometer except for window and cathode. One had a CsI cathode on a 3/8 in. diameter LiF window; the other had a CsTe cathode on a 1 in. diameter sapphire window. The tube with the sapphire window was about 220 times as sensitive to the radiation belts as was the other tube. The spectral responses of these cathodes and transmission curves of the windows are included in Ref. 7.

DESIGN CONSIDERATIONS RELATING TO ENERGETIC PARTICLES

The observations reported here and elsewhere in the literature (Ref. 8) lead to the recognition of the dangers of energetic particles as a cause of loss of transmission and of luminescence in optical systems for space use. Both Hennes and Dunkelman (Ref. 9) and Wolff (Ref. 1) list many references discussing these effects.

The transmission is especially important in the optical elements directly exposed to the radiation. Many, if not most, materials develop absorption bands under exposure to radiation, with certain glasses being far more sensitive than quartz or sapphire. Haynes and Miller (Ref.10) and Heath and Sacher (Ref. 11) investigated the darkening of optical window materials of particular interest to the instrument designer and under typical irradiation for prolonged exposure to the radiation belts.

Secondly, all materials will luminesce under irradiation. Since the flux and spectra of the secondary electrons and x-rays at a specific point within the spacecraft is difficult to predict, it is hard even to determine what tests should be made to check the relative luminescence of various materials. Especially in the ultraviolet, Cerenkov radiation is important, and makes sapphire with its relatively high index of refraction undesireable. Jelley (Ref. 5) is a practical summary of the characteristics and uses of this phenomenon. Mirror surfaces present another set of problems, although aluminum overcoated with MgF_2 appears to be satisfactory for many purposes (Ref. 12).

Careful attention must be given to the window of the photomultiplier. When one considers the proportion of photons which originate in the window and envelope and pass through the photocathode, the arrangement in the EMR side window version is more desireable than that of a semi-transparent cathode on an end window. When one considers Cerenkov radiation, a low index of refraction and as high a value for the short wavelength cut-off as the application permits are desireable. However, the difficulty in making a compact seal between quartz and the envelope of the photomultiplier can make it necessary to use sapphire. With end window tubes, a small effective cathode is desireable, as is inherent in most applications of image dissectors. In any case, adequate shielding of the photomultiplier window and cathode is important.

MODIFICATIONS TO THE MAIN BODY PHOTOMETER

In the Main Body photometer, the principal problem was the effects of energetic particles on the photomultiplier. While it would be desireable to replace the sapphire window with a quartz window (which would also have adequate transmission at 2500A, the shortest wavelength of interest), it was not possible to readily obtain such a photomultiplier that would fit in the space available.

The next best approach is to shield the existing window adequately. To shield along the optical axis, a piece of dynasil, .084" thick was used. To check the effect of this, such a piece was placed .08" in front of the photomultiplier, and the assembly placed in the vacuum tank so that it faced the 1.25 MeV electron beam from the Van de Graaff accelerator. With no electron beam, the dark current in terms of photocathode current was 3×10^{-15} amp; with a beam flux of 6×10^{6} electrons cm^{-2} sec^{-1} the photocathode current was 2.7×10^{-13} amp; and without the dynasil shield, 4.8×10^{-11} amp.

To shield at right angles to the optical axis, the housing for the photomultiplier was redesigned as shown in Figures 17 and 18. In addition to the dynasil shield in front of the photomultiplier, tungsten, .040" thick, and aluminum, .234" thick, were placed around the photocathode and window.

The photometer was taken to the Van de Graaff facility at the Grumman Aircraft Corporation, and tested under conditions similar to the first series of tests at this facility, in a vacuum tank with a beam of 2.6 MeV electrons. A second set of

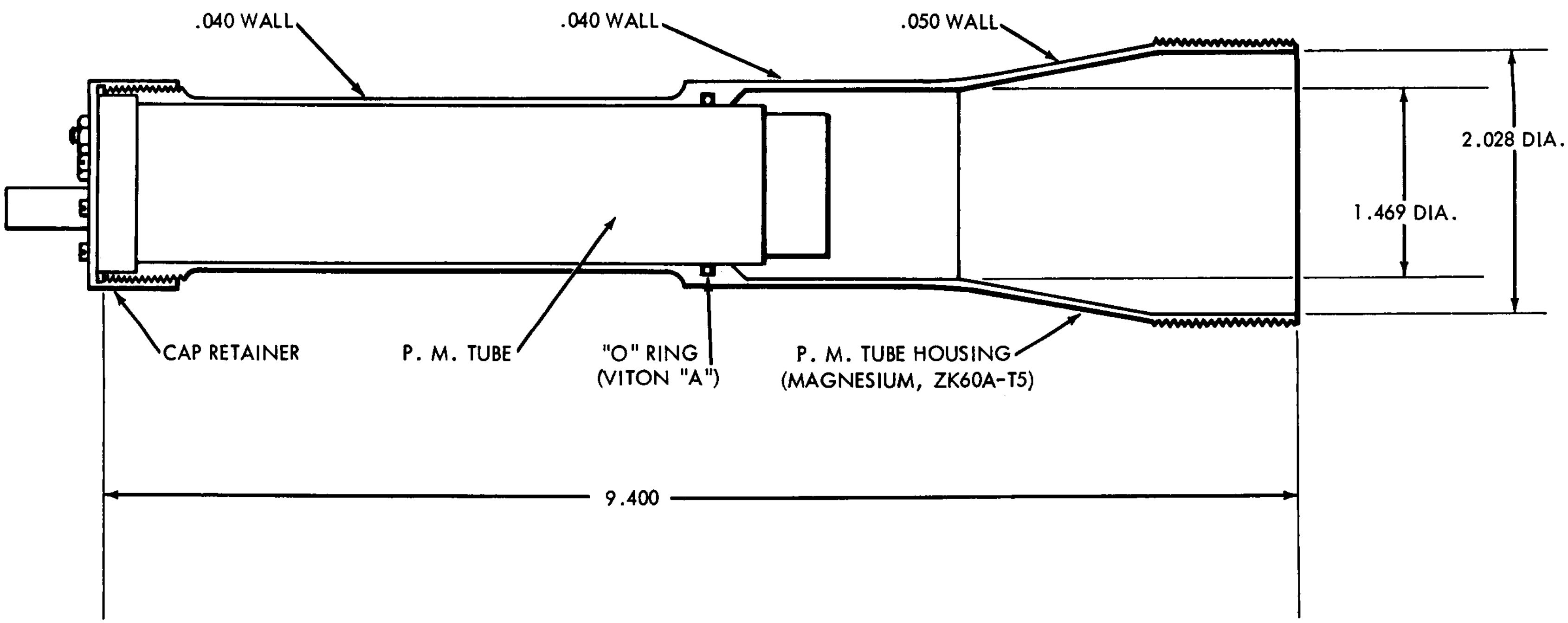

Fig. 17 - The photomultiplier housing in OGO-II

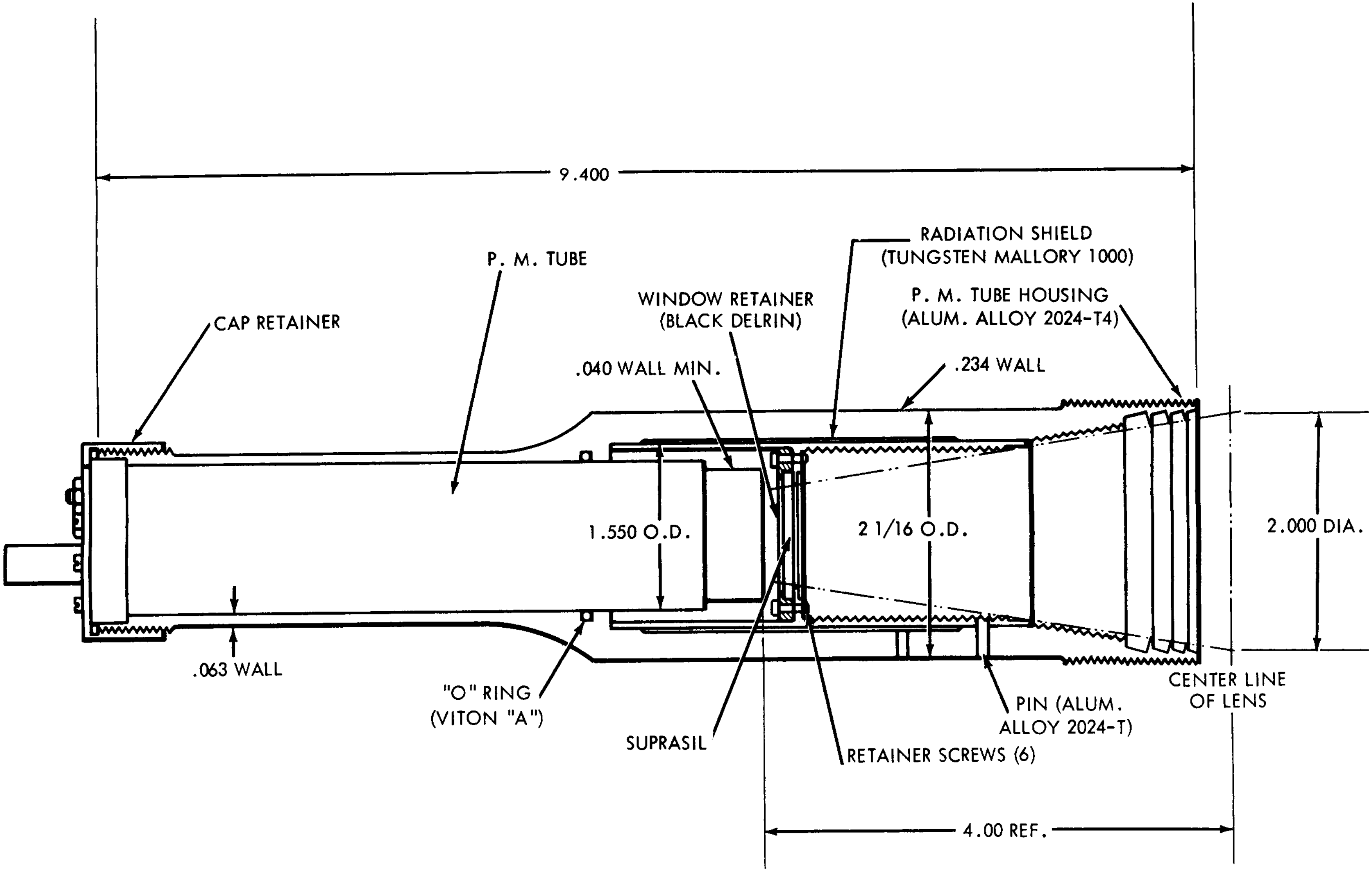

Fig. 18 - The photomultiplier housing as redesigned for OGO-D

tests were also made with the same photometer, but with the old housing. The spacecraft was simulated with sheets of aluminum of various thicknesses. From these data, it appears (Table 8 of the Appendix) that the new housing reduced the sensitivity of the photometer to these electrons by a factor of at least 100.

ACKNOWLEDGEMENTS

Many people have contributed to this investigation. It was through the OAO project office at GSFC that arrangements were made to use the Van de Graaff accelerator at the Grumman Aircraft Corporation at Bethpage, New York. The people who operated this facility, especially A. Favale and M D'Agostina, went out of their way to be helpful. A number of people at GSFC have participated. A. G. Eubanks of the Materials Research and Development Branch set up and conducted the tests using the electron microscope. Dr. D. J. Williams of the Energetic Particles Branch graciously allowed us to interrupt a busy schedule in order to use the Van de Graaff accelerator operated by that Branch. The guidance and support provided by L. Dunkelman and Dr. J. Kupperian of the Astrophysics Branch have made these investigations possible.

REFERENCES

1. C. Wolff, "The Effect of the Earth's Radiation Belts on an Optical System," Applied Optics, 5, 1838-1842, 1966.
2. A. J. Favale, "Large Area Uniform Electron Beams for Space Radiation Environment Studies," in Institute of Environmental Sciences, Annual Technical Meeting, San Diego, Calif., April 13-15, 1966, Proceedings, Institute of Environmental Sciences, Mt. Prospect, Ill., 65-72, (1966).
3. H. A. Zagorites and D. Y. Lee, "Gamma and X-ray-Effects in Multiplier Phototubes, "Naval Radiological Defense Lab., San Francisco, Calif., USNRDL-TR-763, July 7, 1964, AD 603 228.
4. T. P. Sciacca and A. G. Eubanks, "Electron Densitometer for Irradiation Studies in Electron Microscope, "Rev. Sci. Instr., 37, 1019-1020, 1966.
5. J. V. Jelly, "Cerenkov Radiation," Pergamon Press, New York, (1958).
6. C. Barth, University of Colorado (private communication)
7. L. Dunkelman, W. B. Fowler, and J. P. Hennes, "Spectrally Selective Photodetectors for the Middle and Vacuum Ultraviolet," Applied Optics, 1, 695-700, 1962.
8. A. J. Young, "Cosmic Ray Induced Dark Current in Photomultiplier," Rev. Sci. Instr., 37, 1472-1481, 1966.
9. L. Dunkelman and J. Hennes, "Ultraviolet Technology," in The Middle Ultraviolet: Its Science and Technology, A.E.S.Green, Ed., 304-377, J. Wiley and Sons, Inc., New York (1966).

10. G. A. Haynes and W. E. Miller, "Effects of 1.2 and 0.30 Mev Electrons on the Optical Transmission Properties of Several Transparent Materials," NASA TN D2620, March 1965.

11. D. F. Heath and P. A. Sacher, "Effects of a Simulated High Energy Electron Space Environment on the Ultraviolet Transmittance of Optical Materials between 1050 and 3000A, "Applied Optics, 5, 937-943, 1966.

12. L. R. Caufield, G. Hass and J. E. Waylonis, "Further Studies on Mg-F_2 Overcoated Aluminum Mirrors with Highest Reflectance in the Vacuum Ultraviolet", Applied Optics, 5, 45-50, (1966).

APPENDIX

LIST OF TABLES

TABLE 2

LUMINESCENCE OF THE OPTICS

Beam Flux (electrons $cm^{-2}sec^{-1}$)	Photocathode current (amperes)	
	Without Light Stop	With Light Stop
6×10^{6}	6.8×10^{-13}	6.1×10^{-13}
3×10^{7}	3.4×10^{-12}	2.7×10^{-12}
6×10^{7}	6.8×10^{-12}	6.8×10^{-12}
1.2×10^{8}	1.4×10^{-11}	1.4×10^{-11}

Table 2 - Further data from the tests in which 2.6 Mev electrons irradiated the Main Body Photometer. A light stop was placed between the photocathode and the nearest optical element of the photometer.

TABLE 1

EFFECT OF ALUMINUM SHIELDING

Beam Flux (electrons $cm^{-2}sec^{-1}$)	Photocathode current (amperes) for various thicknesses			
	1/32 inch	1/16 inch	1/8 inch	.279 inch
6×10^{5}	3.10×10^{-11}	1.89×10^{-11}	3.48×10^{-12}	
3×10^{6}	1.70×10^{-10}	6.2×10^{-11}	1.29×10^{-11}	
6×10^{6}	2.80×10^{-10}	1.44×10^{-10}	2.81×10^{-11}	
3×10^{7}			1.44×10^{-10}	1.65×10^{-12}
6×10^{7}			2.80×10^{-10}	3.72×10^{-12}
1.2×10^{8}				8.38×10^{-12}
1.8×10^{8}				1.38×10^{-11}

Table 1 - Data resulting from the test in which various thicknesses of aluminum attenuated the 2.6 Mev Electron beam from Grumman's Van de Graaff.

TABLE 3

RESPONSE OF THE PHOTOMULTIPLIER

Beam Flux	Photocathode current (amperes)			
(electrons $cm^{-2}sec^{-1}$)	A	B	C	D
6×10^5				2.6×10^{-11}
3×10^6				8.6×10^{-11}
6×10^6	1.0×10^{-12}	1.0×10^{-12}	1.2×10^{-11}	1.5×10^{-10}
3×10^7	3.2×10^{-12}	3.7×10^{-12}	4.6×10^{-11}	
6×10^7	8.0×10^{-12}	8.0×10^{-12}	8.6×10^{-11}	
1.2×10^8	1.7×10^{-11}	1.7×10^{-11}	1.4×10^{-10}	

Table 3 - Response of various parts of the photomultiplier to 2.6 Mev electrons. Lead is placed as indicated in the correspondingly lettered diagrams of Figure 10 of the main part of this paper.

TABLE 4

VARIOUS SHIELDING CONFIGURATIONS

Beam flux (electrons $cm^{-2}sec^{-1}$)	Photocathode current (amperes)			
	A	B	C	D
6×10^5	8.0×10^{-12}	8.0×10^{-12}		3.9×10^{-14}
3×10^6	4.0×10^{-11}	4.0×10^{-11}	4.0×10^{-11}	2.4×10^{-13}
6×10^6	8.6×10^{-11}	8.6×10^{-11}	8.6×10^{-11}	5.2×10^{-13}
1.8×10^7	2.3×10^{-10}	2.3×10^{-10}	2.3×10^{-10}	1.3×10^{-12}
3×10^7				2.8×10^{-12}
6×10^7				5.4×10^{-12}
1.2×10^8				1.2×10^{-11}
1.8×10^8				1.7×10^{-11}

Table 4 - Response of the photomultiplier to various shield configurations as depicted in the correspondingly lettered diagram of Figure 11 of the main text.

TABLE 5

RESPONSE OF OPEP PHOTOMETER

Beam flux (electrons $cm^{-2}sec^{-1}$)	Photocathode current (amperes) -Y	+Z	-X	+Y	+X
3×10^{7}	1.4×10^{-15}	2×10^{-14}	2.8×10^{-14}	3.4×10^{-14}	3.4×10^{-14}
6×10^{7}	3.2×10^{-15}	4×10^{-14}	5.0×10^{-14}	6.8×10^{-14}	6.8×10^{-14}
1.2×10^{8}	6.4×10^{-15}	8.2×10^{-14}	9.8×10^{-14}	1.5×10^{-13}	1.4×10^{-13}
1.8×10^{8}	1.0×10^{-14}	1.4×10^{-13}	1.6×10^{-13}	2.6×10^{-13}	2.8×10^{-13}

Table 5 - The response of the OPEP photometer to 2.6 Mev electrons. The letters refer to the photometer axis which pointed into the electron beam, as indicated in Figure 12 of the main part of this paper.

TABLE 6

COMPARISON OF PHOTOMULTIPLIERS

(Photocathode current (amperes)

Beam Flux (electrons $cm^{-2}sec^{-1}$)	Serial no. Cathode Dynodes	687 tri-alkali CuBe	660 tri-alkali CuBe	166 Cesium-Antimony AgMg
3×10^{7}		3.4×10^{-14}	4.5×10^{-14}	1.8×10^{-13}
6×10^{7}		6.8×10^{-14}	1.1×10^{-13}	3.4×10^{-13}
1.2×10^{8}		1.4×10^{-13}	2.2×10^{-13}	6.5×10^{-13}
1.8×10^{8}		2.8×10^{-13}	4.5×10^{-13}	9.6×10^{-13}
Gain (1800 volts)		5×10^{5}	3×10^{4}	2.3×10^{5}

Table 6 - Response of two different types of photomultipliers to 2.6 Mev electrons.

TABLE 7

RELATIVE RADIANCE OF DIFFERENT MATERIALS

Material:	Spectrosil	Suprasil II	Dynasil	Corning 9741	Cultured Quartz
Thickness:	.020"	.082"	.084"	.077"	.080"
Beam Flux (electrons $cm^{-2}sec^{-1}$					
6×10^5	.56	.21	.31	.72	.31
6×10^6	3.3	3.5	3.5	5.8	3.3
6×10^7	88	145	127	88	140
6×10^8	780	1400	920	740	960

Material:	Sapphire 108 Insaco	Sapphire 109 Insado	Sapphire	Glass #02.802023	*empty holder
Thickness:	.030"	.030"	.040"	.100"	
Beam Flux (electrons cm-2 sec^{-1}) 0					.12
6×10^5	.39	.46	.44	.24	.13
6×10^6	5.2	6.0	4.2	3.2	.17
6×10^7	187	187	187	127	.38
6×10^8	1960	1570	1570	780	3.2

* This background has been subtracted from the observed signal - the results are as indicated for the various materials.

Table 7 - Relative radiance of different materials when placed in a 1.2 Mev electron beam and viewed in the spectral region between 1600 and 6500A.

TABLE 8

IMPROVED PHOTOMULTIPLIER HOUSING
Photocathode current (amperes)

Beam Flux (electrons $cm^{-2}sec^{-1}$	New Housing with .072" aluminum	New Housing with .125" aluminum	Old housing with .072" aluminum	old housing with .125" aluminum
6×10^{5}			7.8×10^{-11}	1.2×10^{-11}
6×10^{6}	1.9×10^{-12}	3.1×10^{-12}	2.3×10^{-10}	4.6×10^{-11}
3×10^{7}	6.9×10^{-12}	6.9×10^{-12}		1.7×10^{-10}
6×10^{7}	1.1×10^{-11}	1.1×10^{-11}		2.9×10^{-10}
1.2×10^{8}	2.4×10^{-11}	2.4×10^{-11}		
1.8×10^{8}	4.0×10^{-11}	4.0×10^{-11}		

Table 8 - A comparison of the response of the old and new versions of the Main Body photometer to 2.6 Mev electrons. The aluminum is placed in the beam path to simulate the shielding provided by the spacecraft.